Protein Engineering, Design & Selection vol. 24 no. 9 pp. 701–709, 2011
Published online July 13, 2011 doi:10.1093/protein/gzr035

Cell surface display of functional human MHC class II proteins: yeast display versus insect cell display

Fei Wen[1,4], Dhruv K.Sethi[2], Kai W.Wucherpfennig[2] and Huimin Zhao[1,3,5]

[1]Department of Chemical and Biomolecular Engineering, University of Illinois at Urbana-Champaign, Urbana, IL 61801, USA, [2]Department of Cancer Immunology & AIDS, Dana-Farber Cancer Institute and Harvard Medical School, Boston, MA 02115, USA, [3]Departments of Biochemistry, Chemistry, and Bioengineering, Institute for Genomic Biology, University of Illinois at Urbana-Champaign, Urbana, IL 61801, USA and [4]Present address: Department of Microbiology and Immunology, Stanford University, Stanford, CA 94305, USA

[5]To whom correspondence should be addressed.
E-mail: zhao5@illinois.edu

Received February 1, 2011; revised April 26, 2011; accepted June 19, 2011

Edited by Andreas Plueckthun

Reliable and robust systems for engineering functional major histocompatibility complex class II (MHCII) proteins have proved elusive. Availability of such systems would enable the engineering of peptide-MHCII (pMHCII) complexes for therapeutic and diagnostic applications. In this paper, we have developed a system based on insect cell surface display that allows functional expression of heterodimeric DR2 molecules with or without a covalently bound human myelin basic protein (MBP) peptide, which is amenable to directed evolution of DR2–MBP variants with improved T cell receptor (TCR)-binding affinity. This study represents the first example of functional display of human pMHCII complexes on insect cell surface. In the process of developing this pMHCII engineering system, we have also explored the potential of using yeast surface display for the same application. Our data suggest that yeast display is a useful system for analysis and engineering of peptide binding of MHCII proteins, but not suitable for directed evolution of pMHC complexes that bind with low affinity to self-reactive TCRs.

Keywords: directed evolution/DR2–myelin basic protein (MBP)/insect cell display/major histocompatibility complex (MHC)/yeast display

Introduction

With their critical roles in shaping the T cell repertoire and regulating adaptive immune responses, the peptide-major histocompatibility complex (pMHC) complexes, not surprisingly, have been implicated in a number of autoimmune and infectious diseases, cancer and transplantation (Thorsby, 1997; Archbold *et al.*, 2008; Fernando *et al.*, 2008). As a result, there exists much interest in developing pMHC-based therapeutics and diagnostics. For example, recombinant MHC proteins in association with defined peptides have been shown to induce antigen-specific T cell responses *in vitro* (Altman *et al.*, 1993; Kozono *et al.*, 1994). Development of the multimeric forms of these soluble pMHC complexes (commonly known as pMHC tetramers) (Altman *et al.*, 1996) has led to significant advances in the fields of cellular immunology and immunotherapy, enabling direct enumeration, isolation and phenotypic analysis of T cells with defined specificity (Crawford *et al.*, 1998; Meyer *et al.*, 2000), as well as tracking and modulating their responses *in vivo* (Callan *et al.*, 1998; Casares *et al.*, 2002; Maile *et al.*, 2005). Despite such great success, the tetramer technology has been more difficult to use for MHC class II molecules, mainly due to difficulties in production of pMHCII complexes, low avidity of binding between pMHCII and CD4+ T cell receptors (TCR), and the highly polymorphic nature of MHCII genes (Nepom *et al.*, 2002; Vollers and Stern, 2008). While some of these issues could potentially be overcome by design of functional pMHCII complexes with improved TCR-binding affinity (Hackett and Sharma, 2002), the lack of a reliable and high-throughput engineering system remains a technological bottleneck.

Cell surface display coupled with directed evolution has proved powerful in engineering the binding properties of a wide range of proteins including enzymes, antibodies and TCRs (Chen and Georgiou, 2002; Richman and Kranz, 2007; Wen *et al.*, 2008b). To successfully apply this method to the engineering of pMHCII complexes with enhanced TCR-binding affinity, it is critical to display the pMHCII complex in its functional conformation on the cell surface so that fluorescent TCR molecules could be used to enrich and isolate high-affinity pMHCII mutants using fluorescence activated cell sorting (FACS).

As a unicellular eukaryotic host, yeast offers the advantages of possessing post-translational modification machineries and ease of library creation and screening (Boder and Wittrup, 1997; Kondo and Ueda, 2004), thus represents the most attractive display platform organism for engineering mammalian proteins, including the pMHCII complexes (Wen *et al.*, 2009). By using a single-chain construct that covalently fused the extracellular domains of MHCII α- and β-chains, several murine and human MHCII mutants have been successfully displayed on yeast cell surface (Starwalt *et al.*, 2003; Esteban and Zhao, 2004), but no information regarding TCR reactivity was reported. To minimize the possibility that the introduced mutations might alter the TCR binding of the mutant MHCII proteins, Boder *et al.* successfully displayed wild-type DR4–$HA_{307-319}$ and DR1–peptide complexes on yeast cell surface using a non-covalent heterodimeric or trimeric construct, respectively (Boder *et al.*, 2005; Jiang and Boder, 2010). However, the displayed multimeric pMHCII complexes failed to activate T cells or bind TCR tetramers. Using an alternative

display strategy, in which a binding peptide was covalently intercalated between the α- and β-chain of DR1 through two flexible linkers, we recently showed that DR1–peptide complexes could be displayed on yeast cell surface without introduction of any mutations, and the display level correlated with the affinity of the co-expressed peptide (Wen *et al.*, 2008a). More importantly, the resulting DR1–peptide complex was capable of activating T hybridoma cells in a peptide-specific manner, demonstrating for the first time that yeast surface display can be used for T cell epitope identification and potentially for engineering of pMHCII complexes with high TCR-binding affinity.

As a higher eukaryotic host, production of MHCII proteins in baculovirus-infected insect cells has fewer expression or folding problems and usually does not require the introduction of stabilizing mutations which are frequently necessary in yeast. In fact, insect cells are the first reported and currently most widely used expression system for soluble MHCII tetramer preparation and dozens of MHCII alleles from different species have been successfully expressed (Vollers and Stern, 2008). However, the use of insect cell surface display for engineering of MHC proteins has been very limited, largely due to the difficulties in library creation. To date, insect cells have only been used to display murine MHC proteins in complex with peptide libraries for T cell epitope/mimotope identification (Crawford *et al.*, 2006). Nevertheless, the ability of the pMHC complexes displayed on insect cell surface to bind specific TCR tetramers (Crawford *et al.*, 2004; Wang *et al.*, 2005) and elicit protective antitumor immune response *in vivo* (Jordan *et al.*, 2008) also makes this system a promising platform for pMHCII affinity engineering.

Since both yeast and insect surface display systems have shown potential for directed evolution of pMHCII complexes with high TCR-binding affinity, we compared display of a human DR2–MBP_{85-99} complex in both systems, with the aim of establishing a high throughput screening system for pMHCII affinity improvement. The wild-type DR2–MBP complex was not functionally expressed on the yeast cell surface, but mutation of one or two peptide anchor residues that improved binding affinity enabled display of properly folded DR2–peptide complexes. However, none of these mutants showed any TCR reactivity. In contrast, the wild-type DR2–MBP complex was successfully displayed on insect cell surface as either a single-chain or non-covalent heterodimeric protein without the aid of any mutations, and both displayed proteins triggered T cell activation. To our knowledge, this is the first example of functional display of human pMHCII complexes on insect cell surface. More importantly, the displayed heterodimeric DR2–MBP complex bound the TCR tetramer in a peptide-dependent and specific manner, making this system suitable for application for directed evolution of pMHCII complexes with improved TCR-binding affinity.

Materials and methods

Materials

The sequences of all the polymerase chain reaction (PCR) primers are listed in Supplemental Table S1 online and were synthesized by Integrated DNA Technologies (Coralville, IA). T4 DNA ligase, *Phusion* DNA polymerase and all restriction endonucleases were purchased from New England Biolabs (Ipswich, MA). Unless otherwise indicated, all chemicals were purchased from Sigma-Aldrich (St Louis, MO).

Yeast surface display plasmid construction

Plasmid pYD1–DR2–MBP was generated by replacing the DR1β gene in pYD1αMBPβ (Wen *et al.*, 2008a) with the DR2β gene through SpeI/XhoI digestion and ligation. The DR2β gene was obtained by PCR using pPIC–DR2β (Kalandadze *et al.*, 1996) as template and SpeIDR2βFor/DR4βXhoIRev as primer pair. DR2–MBP_{F92Y} was created by ligating a PCR product obtained by using pYD1–DR2–MBP as template and primer pair MBPF4YFor/DR2–XhoIRev into NotI/XhoI digested pYD1–DR2–MBP. DR2–MBP_{V89I}, DR2–MBP_{F92W} and DR2–$MBP_{V89I-F92W}$ were created similarly except that primers MBPF4WFor, MBPV1IFor and MBP1I-4WFor were used in the PCR reactions in place of MBPF4YFor, respectively. $DR2_{\beta P11H}$–MBP was generated by co-transforming a PCR product obtained by using pYD1–DR2–MBP as template and primer pair pYD1For/P11HRev and BstXI/SpeI digested pYD1–DR2–MBP into EBY100 (Invitrogen, Carlsbad, California).

Directed evolution of folded DR2–MBP mutants using yeast surface display

Using pYD1–DR2–MBP as the template and pYD1For/pYD1Rev as primers, error-prone PCR was carried out with 0.15 mM $MnCl_2$. The mutation rate was determined to be ~3 amino acid changes per gene. The error-prone PCR product was then digested with BstXI and SpeI and ligated into pYD1αSTFβ (Wen *et al.*, 2008a). The ligation mixture was transformed into ElectroMax DH5α competent cells (Invitrogen) and a library of 1.7×10^6 clones was obtained. Plasmids were recovered and transformed into EBY100 and a library of 1.8×10^6 clones was generated. After two passages in the selection media SD-CAA (2% dextrose, 0.67% yeast nitrogen base and 1% casamino acids), the library was induced for protein expression using YPG (1% yeast extract, 2% peptone and 2% galactose) and subjected to FACS. The FACS analysis was carried out in the same way as described (Wen *et al.*, 2008a) except that after the third round of enrichment, full-length DR2 variants were selected using anti-V5 antibody (Invitrogen) in the primary staining step. Twelve clones were randomly picked and analyzed individually for their surface display levels. DNA sequencing was carried out to determine the mutations.

Insect cell surface display bacmid construction

The gene encoding the VSVG transmembrane domain was obtained by splicing VSVG2-5 together. The resulting PCR fragment was spliced with another fragment obtained by using pYD1αHAβ(pYD1αHAβ_{L11H}) as the template and gp64SFor/VSVG1Rev as the primer pair, and then ligated into BamHI/EcoRI digested pFastBac plasmid (Invitrogen), yielding the sc-DR1–HA(sc-$DR1_{\beta L11H}$–HA) donor plasmid. The sc-DR2–MBP (sc-$DR2_{\beta L11H}$–MBP) donor plasmid was created by ligating the PCR product, which was obtained by using pYD1αMBPβ as the template and NotIMBPFor(SpeI-P11HFor)/DR2-XhoIRev as the primer pair, into NotI(SpeI)/XhoI digested sc-DR1–HA–SphI plasmid. The DR2α-Fos-encoding gene was obtained by

PCR using pPIC–DR2α (Kalandadze *et al.*, 1996) as the template and NcoI–DRaFor/SphI–FosRev as the primer pair, and then ligated into NcoI/SphI digested pFastBacDual vector (Invitrogen), yielding pFBD–DR2α. The gene encoding DR2β-MBP-Jun-VSVG was obtained by splicing three PCR products: product 1 was obtained by splicing BamHI–MBP1-6, product 2 was obtained by PCR using pPIC–DR2β as the template and DR2b1-7/JunVSVGRev as the primer pair, and product 3 was obtained by splicing VSVG2-4 and VSVGEcoRIRev. The spliced PCR product was then ligated into BamHI/EcoRI digested pFBD–DR2α to generate the LZ–DR2–MBP donor plasmid. The DR2β-Jun-VSVG-encoding gene was obtained by splicing two PCR products: product 1 was obtained by PCR using pPIC–DR2β as the template and w/oMBPFor/JunVSVGRev as the primer pair, and product 2 was obtained by splicing VSVG2-4 and VSVGEcoRIRev. The spliced PCR product was then ligated into BamHI/EcoRI digested pFastBacDual-DR2α to generate the LZ-DR2 donor plasmid. The recombinant bacmid DNA was obtained by transforming the corresponding donor plasmid into DH10Bac (Invitrogen).

Cell surface display and flow cytometric analysis

Saccharomyces cerevisiae EBY100 clones transformed with different yeast surface display plasmids were cultured and analyzed as described (Wen *et al.*, 2008a). For insect cell surface display, the recombinant baculovirus was obtained by Sf9 insect cell transfection of bacmid DNA using Cellfectin II following the manufacturer's protocol (Invitrogen). The P1 viral stock was amplified at least twice to bring the virus titer to $\sim 10^8$ pfu/ml. The multiplicity of infection used for infection was optimized such that the protein display level was high and the cell death rate by day 3 was ~35%. The protein displayed on Sf9 cells was stained and analyzed by flow cytometry as described (Wen *et al.*, 2008a) except that 4,6-diamidino-2-phenylindole (DAPI) was added to the stained cells ~10 min before the analysis to enable gating on live cells.

T cell activation assay

Murine T hybridoma cells 7678 (Call *et al.*, 2009) and HA1.7 (Boen *et al.*, 2000) were used as indicator cell lines for functional DR2–MBP and DR1–HA activity assays, respectively. Both hybridoma cell lines were maintained in IMDM (Invitrogen) with 10% fetal bovine serum at 37°C with 5% CO_2. EBY100 clones displaying different pMHCII complexes were analyzed the same way as described (Wen *et al.*, 2008a). Approximately 10^5 Sf9 cells displaying different pMHCII constructs were washed with phosphate buffered saline (PBS) and co-cultured with $\sim 10^5$ respective indicator T hybridoma cells in a 96-well tissue culture plate for 24 h at 37°C with 5% CO_2. The supernatant was tested for IL-2 production using a murine IL-2 ELISA kit (eBiosciences, San Diego, CA). The B cell line MGAR (Hausmann *et al.*, 1999) was used as a positive control for DR2–MBP presentation. 10 μM of peptide MBP (New England Peptide, Gardner, MA) was added when MGAR or LZ–DR2 was used for antigen presentation.

Preparation of biotinylated Ob.1A12 TCR

The α and β chains of Ob.1A12 TCR were separately cloned into the pET-22b vector (Novagen) and inclusion bodies produced in BL21(DE3) *Escherichia coli* cells (Novagen) were dissolved in 6 M guanidine hydrochloride, 10 mM dithiothreitol and 10 mM EDTA. To initiate refolding, TCR α and β chains were diluted at a 1:1 molar ratio to a concentration of 25 μg/ml of each chain in a refolding buffer containing 5 M urea, 0.5 M L-arginine-HCl, 100 mM Tris-HCl, pH 8.2, 3.7 mM cystamine and 6.6 mM cysteamine. After 40 h at 4°C, the refolding mixture was dialyzed twice against deionized water and twice against 10 mM Tris-HCl, pH 8.0. Refolded TCR was purified by anion exchange chromatography using Poros PI (Applied Biosystems) and MonoQ (GE Healthcare) columns. The interchain disulfide bond located at the C-terminus of the Cα and Cβ Ig domains was moved to the N-terminal part of these domains (replacement of Cα Thr48 and Cβ Ser57 with cysteines) in order to enhance refolding of TCR heterodimer (Boulter *et al.*, 2003). In the expression construct, a BirA tag was placed C-terminal to the TCR β chain. Site-specific biotinylation of the BirA tag was carried out at a protein concentration of 2 mg/ml at a molar ratio of 20:1 (TCR to BirA). Reactions were incubated for 2 h at 30°C in the presence of 100 μM biotin, 10 mM ATP, 10 mM magnesium acetate and protease inhibitors. Excess biotin was removed by dialysis, and biotinylation was confirmed by mobility shift with streptavidin after migration through native polyacrylamide gels.

Tetramer staining

The streptavidin-PE conjugate (BD Biosciences, San Diego, CA) was added to the biotinylated Ob.1A12 TCR (Wucherpfennig *et al.*, 1994) stepwise with 1/10 volume aliquots at room temperature. The resulting tetramer was then diluted to 100 μg/ml for yeast cell staining and 50 μg/ml for insect cell staining. The staining was carried out at 30°C (yeast cell) or 27°C (insect cell) for 2 h and unbound TCR tetramer was washed away three times using PBS. The stained cells were then subjected to flow cytometric analysis.

Results

Yeast surface display of folded single-chain DR2–peptide complexes

The human MHCII protein DR2 (DRA, DRB1*1501) and an epitope of human MBP_{85-99} (ENPVVHFFKNIVTPR) have been implicated in multiple sclerosis (Wucherpfennig *et al.*, 1994). Structural and kinetics studies showed that the Ob.1A12 TCR bound the DR2–MBP_{85-99} complex with an unusual binding topology and a low affinity (Appel *et al.*, 2000; Hahn *et al.*, 2005). Therefore, it would be of both scientific and practical interest to engineer a DR2–MBP variant with improved stability and/or high TCR-binding affinity through directed evolution. To display the wild-type DR2–MBP complex on yeast cell surface for directed evolution experiments, a single-chain construct reported previously was employed (Wen *et al.*, 2008a). As shown in Fig. 1a, the MBP peptide was covalently attached to the C-terminus of the DR2α-chain and N-terminus of the DR2β-chain through two flexible linkers, and expressed on the yeast cell surface as a fusion to the AGA2 protein. The anti-V5 antibody was used to measure the surface display level of the full-length protein, whereas the conformation specific LB3.1 antibody (Stern and Wiley, 1992) was used to

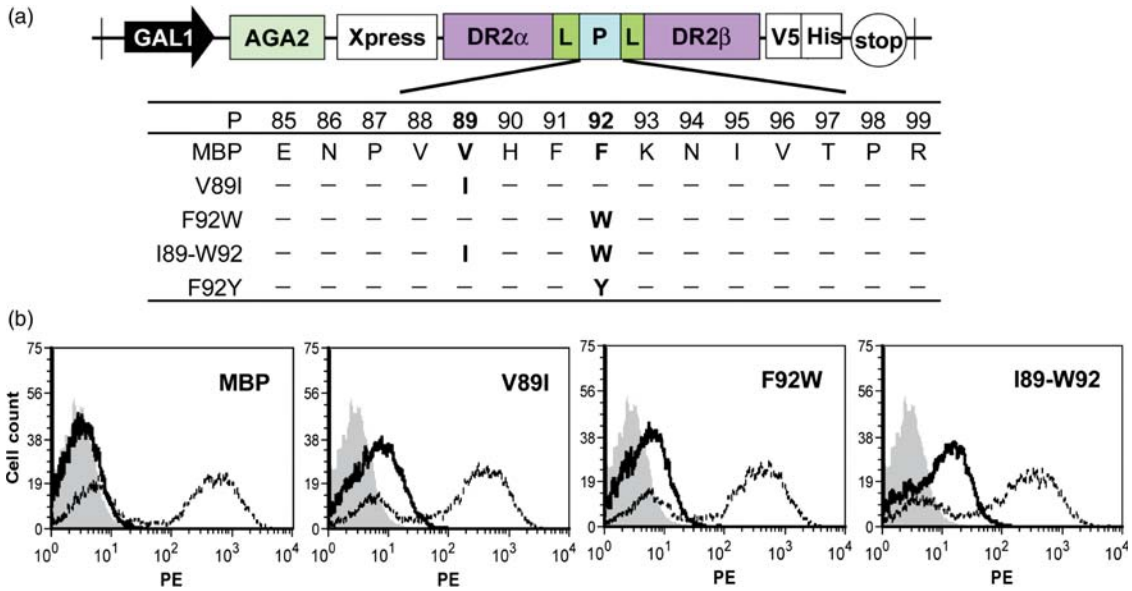

Fig. 1 Design and flow cytometric analysis of single-chain DR2–peptide complexes displayed on yeast cell surface. (**a**) Schematic representation of the single-chain DR2–peptide constructs used for yeast display. The sequences of the intercalating peptide analogs are aligned with MBP_{85-99} and the P1 and P4 anchor residues are highlighted in bold. GAL1, yeast GAL1 promoter; AGA2, an adhesion subunit of the yeast α-agglutinin protein (Boder and Wittrup, 1997); Xpress, Xpress epitope; L, linker; P, peptide; V5, V5 epitope; His, His_6 tag. (**b**) Flow cytometric analysis of yeast surface displayed DR2–peptide complexes. Yeast cells were stained with anti-V5 antibody to detect full-length protein expression (dashed line) or with conformation specific LB3.1 antibody to detect correctly folded protein (solid line). Yeast cells transformed with empty pYD1 plasmid stained with LB3.1 were used as negative control (shade). The histograms are representative of at least three independent experiments.

detect correctly assembled DR2 protein. Flow cytometric analysis of yeast cells expressing the DR2–MBP construct showed a positive population with the anti-V5 antibody, but only a weak LB3.1 staining signal similar to that of the control yeast strain transformed with an empty vector (Fig. 1b, panel MBP). This result suggested that the DR2–MBP protein was displayed on yeast cell surface in full length, but not correctly assembled.

Previously, we observed a positive correlation between the peptide-binding affinity and the yeast surface display level of the resulting peptide–DR1 complex as measured by LB3.1 antibody staining (Wen *et al.*, 2008a). Based on this finding, we hypothesized that co-expressing a peptide with higher DR2-binding affinity than MBP would enable the display of correctly folded wild-type DR2. To test this hypothesis, we designed three yeast surface display constructs containing peptides that differ from the MBP_{85-99} peptide at the P1 (V89) and/or P4 (F92) major anchor residues (Fig. 1a). The mutations of V89→I and F92→W were chosen because they have been shown to increase the binding affinity toward DR2 (Belmares *et al.*, 2002). As expected, the MBP peptide analog MBP_{V89I} or MBP_{F92W} with a single mutation enabled the yeast surface expression of folded DR2, although the improvement was modest and accounted for only a small fraction of the total protein (Fig. 1b). The display level of the LB3.1-reactive DR2 protein was further increased when both mutations were combined (peptide $MBP_{I89-W92}$, Fig. 1b and 2d), suggesting that the two anchor residue mutations have an additive effect in stabilizing the native conformation of DR2 on yeast cell surface. Taken together, these data suggest that, in addition to the DR1 and DR4 alleles (Wen *et al.*, 2008a), yeast cells were also able to display properly folded DR2 protein when a peptide with high binding affinity was co-expressed, indicating the general applicability of the single-chain pMHCII display strategy as depicted in Fig. 1a. Although assembled into their native forms, the displayed complexes formed between the DR2 protein and MBP peptide analogs failed to react with the DR2–MBP-specific TCR tetramer or T cell hybridoma (Supplemental Fig. S1), thus could not be used as the template for directed evolution of pMHCII complexes with improved TCR-binding affinity. This failure of yeast displayed DR2–peptide complexes to engage TCR might be a result of their low expression level, since a large fraction of the total protein on the cell surface was not correctly folded (Fig. 1b). The display level is likely to be critical, given the low affinity of Ob.1A12 TCR for the DR2–MBP complex. It is also possible that the two mutations abolished TCR recognition of the complex. To address this issue, we carried out directed evolution experiments to isolate folded DR2–MBP variants with improved yeast surface display level.

Directed evolution of folded DR2–MBP variants using yeast surface display

A library of DR2–MBP variants was created by error-prone PCR and screened by FACS using the conformation sensitive antibody, LB3.1. As shown in Fig. 2a, after three rounds of cell sorting, there was a significant enrichment of folded variants with improved display level. Twelve clones with full-length genes were randomly selected and sequenced. The alignment with the wild-type DR2–MBP sequence revealed two interesting mutations (highlighted in Fig. 2b): the first one was a phenylalanine to tyrosine mutation at the P4 anchor residue of the MBP peptide (MBP_{F92Y}), which has been shown to favor aromatic as well as aliphatic residues (Wucherpfennig *et al.*, 1994; Smith *et al.*, 1998); the second was a proline to histidine mutation at the β11 position, which was present in 7 of the 12 isolated clones and also

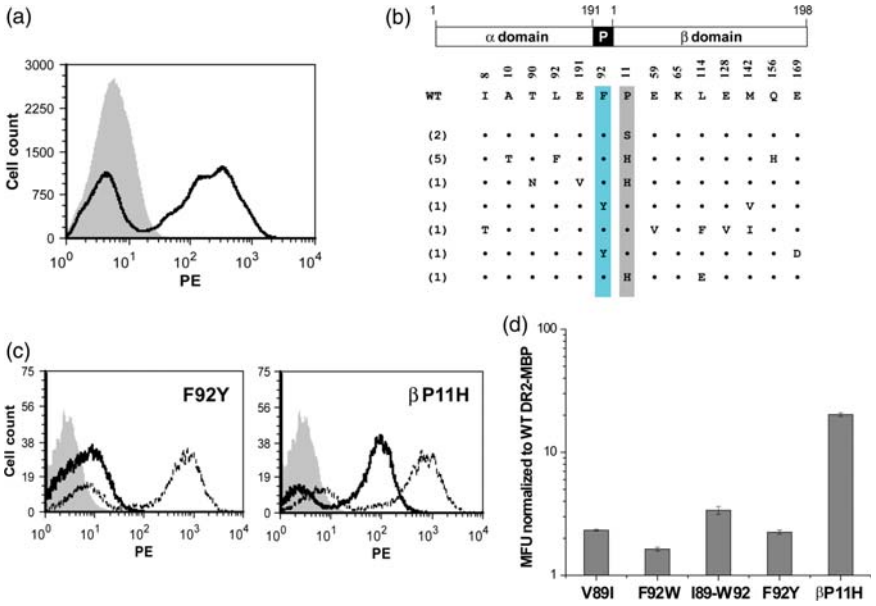

Fig. 2 Engineering of correctly folded DR2–MBP variants using directed evolution and yeast surface display. (**a**) FACS enrichment of DR2–MBP variants with improved surface display level from a random mutagenesis library. The yeast cells were stained with conformation specific LB3.1 antibody. Histograms of the display library before and after three rounds of enrichment are shown in shade and solid line, respectively. (**b**) Sequence alignment of the evolved variants with the wild-type DR2–MBP. The number of independent isolates of each clone is shown in parentheses. (**c**) Flow cytometric analysis of yeast surface displayed DR2–MBP_{F92Y} and $DR2_{\beta P11H}$–MBP complexes. The data are presented the same way as described in Fig. 1b. (**d**) Relative surface display levels of correctly assembled DR2–MBP mutants to that of the wild-type protein as measured by LB3.1 antibody staining. MFU, mean fluorescence unit.

found to be important for the proper folding of DR1 on the yeast cell surface (Esteban and Zhao, 2004). To minimize the number of introduced mutations and thus their potential of altering TCR interaction, two single mutants were constructed: DR2–MBP_{F92Y} and DR2 $_{\beta P11H}$–MBP. As shown in Fig. 2c and d, the MBP_{F92Y} mutation only had a modest stabilizing effect similar to that of MBP_{V89I} and MBP_{F92W}, whereas the βP11H mutation significantly increased the expression level of the folded DR2 protein. Unfortunately, both DR2–MBP_{F92Y} and $DR2_{\beta P11H}$–MBP, although displayed in their native conformation, failed to engage DR2–MBP-specific TCR (Supplemental Fig. S1).

Insect cell surface display of functional single-chain DR2–MBP complexes

Recent studies have shown that a murine pMHCII complex IA^b-p3K displayed on insect cell surface activated specific T hybridoma cells and bound TCR tetramers stably (Crawford *et al*., 2004). Therefore, we decided to test whether it was suitable for the human DR2–MBP complex. The gene encoding the wild-type single-chain DR2α–MBP–DR2β used for yeast surface display (Fig. 1a) was expressed as an N-terminal fusion to the VSVG anchor protein (referred as sc-DR2–MBP henceforward). As shown in Fig. 3a, the sc-DR2–MBP polypeptide was displayed and correctly assembled on Sf9 insect cell surface as evidenced by positive staining with the LB3.1 antibody. Interestingly, while the βP11H mutation significantly improved the display level of folded DR2 protein on yeast cell surface (Fig. 2c and d), it actually resulted in a slightly lower display level than wild-type sc-DR2–MBP on the insect cell surface, and a more substantial decrease was observed in the case of DR1–HA (Fig. 3a). These results indicate that the stabilizing effect of βP11H might be unique to the yeast expression system, thus additional biochemical characterization using purified protein might be necessary in the future for analyzing how mutations identified from a yeast display library contribute to pMHCII structural stability.

Two approaches were then used to examine TCR binding of the displayed sc-DR2–MBP complex, activation of a T cell hybridoma and TCR tetramer staining. For the T cell activation assay, the murine T cell hybridoma 7678 which recognizes the DR2–MBP complex (Call *et al*., 2009) was used as an indicator cell line for productive pMHC–TCR interaction that leads to IL-2 secretion. Another two human pMHCII constructs, sc-DR1–HA and sc-$DR1_{\beta P11H}$–HA, both of which were also successfully displayed in their native forms (Fig. 3a), were generated and used as negative controls. As shown in Fig. 3b, the wild-type sc-DR2–MBP complex displayed on insect cell surface induced IL-2 secretion by the 7678 T cell hybridoma, while the sc-$DR2_{\beta P11H}$–MBP mutant triggered a weak response with an IL-2 secretion level that was ~2-fold above background. More importantly, the 7678 hybridoma did not respond to insect cells displaying the sc-$DR1_{\beta P11H}$–HA complexes or expressing the empty bacmid. Note that both sc-DR1–HA and sc-$DR1_{\beta P11H}$–HA complexes were also capable of stimulating a DR1–HA-specific T cell hybridoma HA1.7 (Boen *et al*., 2000) to secrete ~500 and ~700 pg/ml of IL-2, respectively (Supplemental Fig. S2a). Taken together, these data suggest a productive and specific interaction between the displayed sc-DR2–MBP complex and the TCR on 7678 cells. However, to our surprise, no TCR tetramer staining was observed with any of the constructs (Supplemental Fig. S2b), which may be due to the low affinity of Ob.1A12 TCR binding to DR2–MBP. Similar discrepancy has been reported in several other studies where soluble pMHCII tetramer could activate, but not stain T cells, and the reason is not yet clear (Vollers and Stern, 2008). We hypothesized that, in our case, the density of the DR2–MBP complex on

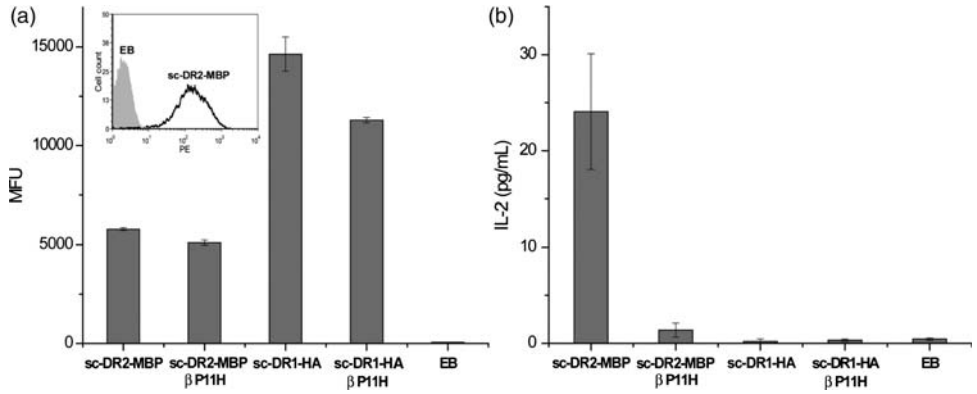

Fig. 3 Characterization of insect cell surface displayed single-chain pMHCII constructs. (**a**) Flow cytometric analysis. The conformation specific LB3.1 antibody was used for staining and the histograms of insect cells infected with wild-type baculovirus (shade) and with recombinant sc-DR2–MBP baculovirus (solid line) are shown in the inset. (**b**) T cell hybridoma activation analysis. The average and standard deviation of the IL-2 concentration obtained from triplicate experiments are plotted. EB, empty bacmid (i.e. wild-type baculovirus).

insect cell surface would be a very important factor in forming a stable TCR tetramer binding because of the low affinity of the monomeric interaction (Appel *et al.*, 2000). To increase display density, we decided to include the leucine zipper dimerization domains (Kalandadze *et al.*, 1996) to promote assembly of a native αβ heterodimer. It should be noted that, although the use of leucine zipper dimerization motifs allowed the assembly and secretion of soluble empty DR2 protein in *Pichia pastoris*, it did not enable functional expression of DR2–MBP complex on the surface of the yeast display strain *S.cerevisiae* in this study (data not shown).

Leucine zipper enhanced functional display of DR2 protein on insect cell surface

The leucine zipper dimerization motifs from the transcription factors Fos and Jun were fused to the C-terminus of the DR2α- and DR2β-chain, respectively, as reported previously (Kalandadze *et al.*, 1996). In addition, the MBP peptide and the VSVG anchor protein were attached to the N- and C-terminus of the DR2β-Jun polypeptide, respectively. To display the heterodimeric DR2–MBP complexes (referred as LZ–DR2–MBP henceforward), the resulting DR2α-Fos and MBP-DR2β-Jun-VSVG cassettes were co-expressed in insect cells under the control of ph and p10 promoters, respectively. Since the leucine zipper has been shown to enable the assembly of empty DR2 (Kalandadze *et al.*, 1996), a LZ–DR2 construct, which contained the DR2α-Fos and DR2β-Jun-VSVG cassettes, was made to examine if it could also be functionally displayed on insect cell surface. As shown in Fig. 4a, the use of leucine zipper indeed improved the display level of properly assembled DR2–MBP heterodimers with ∼2.5-fold higher mean fluorescence units (MFU) than the sc-DR2–MBP construct. In addition, it also enabled correct assembly and display of DR2 protein in the absence of a covalently linked MBP peptide. Compared to LZ–DR2–MBP, the LZ–DR2 construct even showed a slightly higher display level, indicating that a linked peptide was not required for display of DR2 protein in the presence of the leucine zipper.

The T cell activation assay was carried out next to evaluate the function of the leucine zipper constructs. Reflective of its improved surface display level, the LZ–DR2–MBP complex induced 7678 hybridoma to secrete IL-2 at a much higher level (134 pg/ml) than sc-DR2–MBP (24 pg/ml) (Fig. 4b). Compared to a professional antigen presenting cell, MGAR (a human B cell line homozygous for DR2 (Hausmann *et al.*, 1999)), insect cells displaying the LZ–DR2–MBP complex only showed ∼30% less IL-2 induction, demonstrating a high antigen presentation efficiency. As shown in Fig. 4b, the LZ–DR2 construct did not activate 7678 hybridoma cells unless free MBP peptide was supplemented. Although the response was much weaker than LZ–DR2–MBP, this result clearly indicated that the empty DR2 heterodimer was capable of binding the MBP peptide to form an active TCR ligand. Taken together, these data demonstrate that both the LZ–DR2–MBP and LZ–DR2 complexes displayed on the insect cell surface were functional and engaged the TCRs on 7678 T cell hybridoma in an epitope-dependent manner.

With the success of increasing the display density of functional DR2–MBP complexes on insect cell surface, the LZ–DR2–MBP construct was further examined for its ability to bind a tetrameric form of the Ob.1A12 TCR. The LZ–DR2 and sc-DR1–HA cells were also included as negative controls. As shown in Fig. 4c, left panel and d, the Ob.1A12 TCR tetramer bound to insect cells displaying LZ–DR2–MBP, but not to negative control cells. The staining by this tetramer was lower than previously observed for the murine IA^b-p3K system (Crawford *et al.*, 2004), which was expected because of the low affinity of purified Ob.1A12 TCR and DR2–MBP determined in surface plasmon resonance studies (Appel *et al.*, 2000). Although the expression of LZ–DR2–MBP was fairly homogeneous (Fig. 4a, inset), this low affinity also resulted in a very heterogeneous tetramer binding of insect cells displaying LZ–DR2–MBP (Fig. 4c). When the LB3.1 antibody and the TCR tetramer were used simultaneously for surface staining, cells with similar LZ–DR2–MBP display levels showed a large degree of variation of TCR tetramer binding (Fig. 4c, right panel), suggesting that there was no direct correlation between the LZ–DR2–MBP surface display level and the Ob.1A12 tetramer staining (Fig. 4c, right panel), which was observed for the murine IA^b-p3K system (Crawford *et al.*, 2004). Overall, these data strongly suggest that the LZ–DR2–MBP complex displayed on the

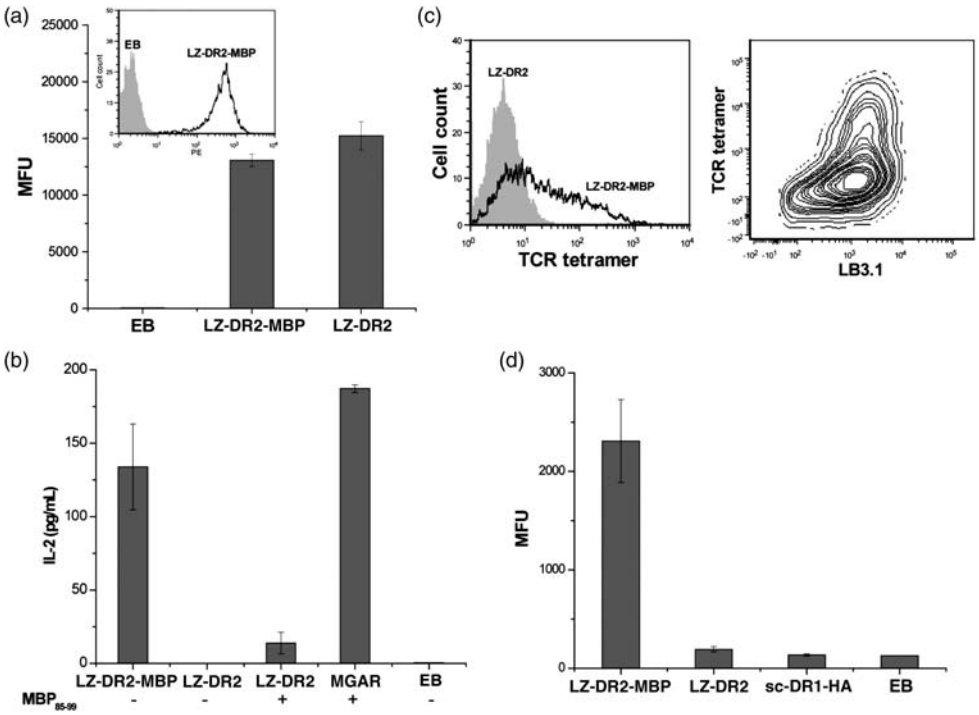

Fig. 4 Characterization of insect cell surface displayed leucine zipper constructs. The flow cytometric (**a**) and T cell hybridoma activation (**b**) analysis results are presented the same way as described in Fig. 3a and b, respectively. In the T cell hybridoma activation assay, a MGAR B cell line was included as a positive control for antigen presentation and soluble MBP_{85-99} peptide was added exogenously. (**c**) TCR tetramer staining analysis. Insect cells displaying LZ–DR2 and LZ–DR2–MBP were stained with Ob.1A12 TCR tetramer, and the resulting histograms are shown in shade and solid line, respectively (left panel). The insect cells displaying LZ–DR2–MBP were simultaneously stained with TCR tetramer and LB3.1 antibody, and the resulting contour plot is shown with biexponential scaling (right panel). (**d**) The column chart representation of the Ob.1A12 TCR tetramer staining results.

insect cell surface was capable of specifically binding Ob.1A12 TCR tetramers in a peptide-dependent manner.

Discussion

Human major histocompatibility complex (MHC) proteins bind peptides derived from self or foreign proteins and present them on the surface of antigen presenting cells for surveillance by T cells (Stern and Wiley, 1994; Strominger and Wiley, 1995; Gascoigne *et al.*, 2001). T cell responsiveness to the peptide is affected by both its affinity for the presenting MHC molecule and the affinity of the pMHC complex for TCR (Slansky *et al.*, 2000). Hence, reliable and robust systems for isolating MHC-binding peptides and engineering pMHC complexes with improved TCR-binding affinity are highly desirable for applications ranging from structure–function study to therapeutics design. In an effort to develop such a system, we explored two display platforms – yeast and insect cell surface display (Crawford *et al.*, 2004; Wen *et al.*, 2008a).

Previously, we have successfully displayed functional sc-DR1 protein on yeast cell surface by co-expression with the high-affinity $HA_{306-318}$ peptide (Wen *et al.*, 2008a). Although the same strategy did not work for wild-type DR2–MBP_{85-99}, co-expressing MBP peptide analogs with higher DR2-binding affinity (MBP_{V89I}, MBP_{F92W} and $MBP_{I89-W92}$) enabled display of correctly assembled DR2 on the yeast cell surface at a level that was reflective of their binding affinity (Figs 1 and 2d). This is the second example demonstrating a positive correlation between the peptide-binding affinity and the display level of the resulting pMHCII complex on yeast cell surface, the first one being DR1 (Wen *et al.*, 2008a). As another supporting evidence, the directed evolution experiment carried out later with the aim to isolate stabilized DR2–MBP variants also revealed a mutant expressing a high-affinity peptide, MBP_{F92Y} (Fig. 2). In an elegant study published recently, Boder and coworkers have adapted the classical yeast display system to allow a peptide-binding-dependent co-display of non-covalent trimeric DR1–peptide complexes (Jiang and Boder, 2010). Their results further demonstrated the astonishing ability of yeast to quantitatively distinguish the peptide affinity for DR1 paralleling that of *in vitro* competitive binding assays and bioinformatics approaches. Taken together, these data strongly suggested that yeast display is a reliable system for peptide-binding analysis of human MHCII proteins. Coupled with peptide library creation and screening, T cell epitopes (Wen *et al.*, 2008a), mimotopes (Jiang and Boder, 2010) or altered peptide ligands with high MHCII-binding affinity should be readily identified in a high throughput manner.

In addition to their high DR2-binding affinity, the four MBP peptide analogs were designed to contain mutations at non-TCR contacting residues P1 and/or P4 to avoid disrupting the pMHCII–TCR interaction, but it is well known that mutations at anchor residues can disrupt TCR binding. For the same reason, mutation βP11H, which is located on the first β-strand of the β1 domain lining the bottom of the P6 binding pocket (Hahn *et al.*, 2005), was selected among the others identified from the random mutagenesis study (Fig. 2). Despite these considerations, the yeast cells displaying the aforementioned five complexes failed to induce DR2–MBP-specific 7678 T hybridoma cell response or bind

Ob.1A12 TCR tetramer (Supplemental Fig. S1). T cell stimulation data obtained with insect cells displaying the sc-DR2$_{\beta P11H}$–MBP complex, however, clearly showed that the mutation βP11H did not abolish its interaction with the specific TCR, although it might have some negative effect, as the wild-type sc-DR2–MBP triggered a stronger T cell response (Fig. 3b). Additionally, peptide MBP$_{F92W}$ has been shown to induce similar or even higher response than the wild-type MBP peptide (Wucherpfennig *et al.*, 1994). Therefore, the inability of the recombinant yeast cells to activate 7678 T hybridoma cells suggested some intrinsic limitations of using yeast cells for antigen presentation. Further supporting this statement, yeast cells displaying the wild-type DR1–HA complex could not activate its specific T hybridoma cell that has been engineered to have increased sensitivity unless they were immobilized on a plastic surface (Wen *et al.*, 2008a). The exact molecular mechanism accounting for the limited success of using yeast for antigen presentation has yet to be determined. One possibility is that since the displayed pMHC complexes are spatially distributed on the yeast cell surface, it might require an extremely high expression level to reach a pMHC density threshold that supports a stable TCR interaction, especially for pMHC class II complexes that in general exhibit lower TCR affinity than class I (Cole *et al.*, 2007). In any case, significant re-engineering efforts are required to enable the use of yeast surface display for engineering TCR reactivity of pMHCII complexes.

To date, there are few studies using insect cell surface display for pMHCII engineering and they are limited to several murine alleles (Crawford *et al.*, 2006). We demonstrated here that human pMHCII complexes could also be functionally displayed on insect cell surface (Figs 3 and 4). Two different expression strategies were tested for displaying the DR2–MBP complex on insect cell surface: single-chain (sc-DR2–MBP) and non-covalent heterodimer (LZ–DR2–MBP) constructs. Both designs exhibited surface display of the DR2–MBP complex in a form that could be recognized by conformation specific LB3.1 antibody and DR2–MBP-specific 7678 T cell hybridoma. However, only the LZ–DR2–MBP construct showed binding of specific Ob.1A12 TCR tetramer. This result could be partly explained by the higher display level of the LZ–DR2–MBP complex (Figs 3a and 4a), which might be critical for tetramer binding. In addition, the crystal structure of DR2-MBP-Ob.1A12 revealed a very unusual topology, in which the TCR was shifted to the N-terminal end of the MBP peptide in the DR2-binding site, making contact with the backbone of E85 at the P-4 position (Hahn *et al.*, 2005). As a result, the linker at the N-terminus of the MBP peptide in the sc-DR2–MBP construct might create some steric hindrance to TCR binding; thus, its removal in the leucine zipper version may have allowed a more stable interaction between the LZ–DR2–MBP complex and the soluble Ob.1A12 TCR tetramer.

More importantly, we have also demonstrated in this work that the Ob.1A12 TCR tetramer only showed staining of insect cells displaying the LZ–DR2–MBP, but not of those displaying empty LZ–DR2 protein or unrelated DR1–HA complexes (Fig. 4c and d). This peptide-dependent TCR tetramer binding allows the use of the described insect cell display system for differentiating DR2–MBP variants that bind TCR tetramer tightly from those that bind weakly. Coupled with directed evolution and FACS, DR2 variants with high TCR-binding affinity could in the future be readily identified from a mutagenesis library in a high throughput manner. Meanwhile, it should be noted that the generation of a protein library in insect cells with a sufficient diversity to cover the necessary sequence space is not a trivial task. The standard library creation method usually requires the preparation of a donor plasmid library in *E.coli*, followed by co-transfection with linearized baculovirus DNA into insect cells. The low cell transformation/transfection efficiency is a limiting factor, which results in a small library size of $<10^5$ (Crawford *et al.*, 2004). However, by directly introducing *in vitro* ligated recombinant baculovirus DNA into insect cells, a recent study has shown that a library of up to 10^8 independent variants could be generated (Crawford *et al.*, 2006), reaching the limit of *in vivo* cell-based library creation techniques (Aharoni *et al.*, 2005). This result further demonstrated the feasibility of using insect cell surface display as a protein engineering platform. Currently, we have created a random mutagenesis library of DR2–MBP variants using the described insect cell display system and library screening is in progress.

To our knowledge, *in vitro* evolution of pMHCII complexes with improved TCR-binding affinity has not been reported due to the lack of a high throughput engineering system. The development of the described insect cell display system in this work could potentially lead to the identification of such mutants. Although yet to be demonstrated, we envision that the engineered pMHCII complexes with high affinity towards TCR could be of clinical value. For example, they could be used directly as staining reagents to monitor the behavior of T cells with improved sensitivity.

Supplementary data

Supplementary data are available at *PEDS* online.

Acknowledgements

We thank D.M. Kranz (University of Illinois) for helpful discussions and suggestions; M. Schuler and Z. Wen (University of Illinois) for advice on insect cell cloning and culture; B. Pilas and B. Montez at the Biotechnology Center of the University of Illinois for flow cytometry and FACS assistance.

Funding

This work was supported by the Department of Chemical and Biomolecular Engineering of the University of Illinois at Urbana-Champaign and grants from the National Institutes of Health to K.W.W. (PO1 AI045757, R01AI054520).

References

Aharoni,A., Griffiths,A.D. and Tawfik,D.S. (2005) *Curr. Opin. Chem. Biol.*, **9**, 210–216.

Altman,J.D., Moss,P.A., Goulder,P.J., Barouch,D.H., McHeyzer-Williams,M.G., Bell,J.I., McMichael,A.J. and Davis,M.M. (1996) *Science*, **274**, 94–96.

Altman,J.D., Reay,P.A. and Davis,M.M. (1993) *Proc. Natl Acad. Sci. U S A*, **90**, 10330–10334.

Appel,H., Gauthier,L., Pyrdol,J. and Wucherpfennig,K.W. (2000) *J. Biol. Chem.*, **275**, 312–321.

Archbold,J.K., Ely,L.K., Kjer-Nielsen,L., Burrows,S.R., Rossjohn,J., McCluskey,J. and Macdonald,W.A. (2008) *Mol. Immunol.*, **45**, 583–598.

Belmares,M.P., Busch,R., Wucherpfennig,K.W., McConnell,H.M. and Mellins,E.D. (2002) *J. Immunol.*, **169**, 5109–5117.
Boder,E.T., Bill,J.R., Nields,A.W., Marrack,P.C. and Kappler,J.W. (2005) *Biotechnol. Bioeng.*, **92**, 485–491.
Boder,E.T. and Wittrup,K.D. (1997) *Nat. Biotechnol.*, **15**, 553–557.
Boen,E., Crownover,A.R., McIlhaney,M., Korman,A.J. and Bill,J. (2000) *J. Immunol.*, **165**, 2040–2047.
Boulter,J.M., Glick,M., Todorov,P.T., Baston,E., Sami,M., Rizkallah,P. and Jakobsen,B.K. (2003) *Protein Eng.*, **16**, 707–711.
Call,M.J., Xing,X., Cuny,G.D., Seth,N.P., Altmann,D.M., Fugger,L., Krogsgaard,M., Stein,R.L. and Wucherpfennig,K.W. (2009) *J. Immunol.*, **182**, 6342–6352.
Callan,M.F., Tan,L., Annels,N., Ogg,G.S., Wilson,J.D., O'Callaghan,C.A., Steven,N., McMichael,A.J. and Rickinson,A.B. (1998) *J. Exp. Med.*, **187**, 1395–1402.
Casares,S., Hurtado,A., McEvoy,R.C., Sarukhan,A., von Boehmer,H. and Brumeanu,T.D. (2002) *Nat. Immunol.*, **3**, 383–391.
Chen,W. and Georgiou,G. (2002) *Biotechnol. Bioeng.*, **79**, 496–503.
Cole,D.K., Pumphrey,N.J., Boulter,J.M., *et al*. (2007) *J. Immunol.*, **178**, 5727–5734.
Crawford,F., Huseby,E., White,J., Marrack,P. and Kappler,J.W. (2004) *PLoS Biol.*, **2**, E90.
Crawford,F., Jordan,K.R., Stadinski,B., Wang,Y., Huseby,E., Marrack,P., Slansky,J.E. and Kappler,J.W. (2006) *Immunol. Rev.*, **210**, 156–170.
Crawford,F., Kozono,H., White,J., Marrack,P. and Kappler,J. (1998) *Immunity*, **8**, 675–682.
Esteban,O. and Zhao,H. (2004) *J. Mol. Biol.*, **340**, 81–95.
Fernando,M.M., Stevens,C.R., Walsh,E.C., De Jager,P.L., Goyette,P., Plenge,R.M., Vyse,T.J. and Rioux,J.D. (2008) *PLoS Genet.*, **4**, e1000024.
Gascoigne,N.R., Zal,T. and Alam,S.M. (2001) *Expert Rev. Mol. Med.*, **2001**, 1–17.
Hackett,C.J. and Sharma,O.K. (2002) *Nat. Immunol.*, **3**, 887–889.
Hahn,M., Nicholson,M.J., Pyrdol,J. and Wucherpfennig,K.W. (2005) *Nat. Immunol.*, **6**, 490–496.
Hausmann,S., Martin,M., Gauthier,L. and Wucherpfennig,K.W. (1999) *J. Immunol.*, **162**, 338–344.
Jiang,W. and Boder,E.T. (2010) *Proc. Natl Acad. Sci. U S A*, **107**, 13258–13263.
Jordan,K.R., McMahan,R.H., Oh,J.Z., Pipeling,M.R., Pardoll,D.M., Kedl,R.M., Kappler,J.W. and Slansky,J.E. (2008) *J. Immunol.*, **180**, 188–197.
Kalandadze,A., Galleno,M., Foncerrada,L., Strominger,J.L. and Wucherpfennig,K.W. (1996) *J. Biol. Chem.*, **271**, 20156–20162.
Kondo,A. and Ueda,M. (2004) *Appl. Microbiol. Biotechnol.*, **64**, 28–40.
Kozono,H., White,J., Clements,J., Marrack,P. and Kappler,J. (1994) *Nature*, **369**, 151–154.
Maile,R., Siler,C.A., Kerry,S.E., Midkiff,K.E., Collins,E.J. and Frelinger,J.A. (2005) *J. Immunol.*, **174**, 619–627.
Meyer,A.L., Trollmo,C., Crawford,F., Marrack,P., Steere,A.C., Huber,B.T., Kappler,J. and Hafler,D.A. (2000) *Proc. Natl Acad. Sci. U S A*, **97**, 11433–11438.
Nepom,G.T., Buckner,J.H., Novak,E.J., Reichstetter,S., Reijonen,H., Gebe,J., Wang,R., Swanson,E. and Kwok,W.W. (2002) *Arthritis Rheum.*, **46**, 5–12.
Richman,S.A. and Kranz,D.M. (2007) *Biomol. Eng.*, **24**, 361–373.
Slansky,J.E., Rattis,F.M., Boyd,L.F., Fahmy,T., Jaffee,E.M., Schneck,J.P., Margulies,D.H. and Pardoll,D.M. (2000) *Immunity*, **13**, 529–538.
Smith,K.J., Pyrdol,J., Gauthier,L., Wiley,D.C. and Wucherpfennig,K.W. (1998) *J. Exp. Med.*, **188**, 1511–1520.
Starwalt,S.E., Masteller,E.L., Bluestone,J.A. and Kranz,D.M. (2003) *Protein Eng.*, **16**, 147–156.
Stern,L.J. and Wiley,D.C. (1992) *Cell*, **68**, 465–477.
Stern,L.J. and Wiley,D.C. (1994) *Structure*, **2**, 245–251.
Strominger,J.L. and Wiley,D.C. (1995) *JAMA*, **274**, 1074–1076.
Thorsby,E. (1997) *Human Immunol.*, **53**, 1–11.
Vollers,S.S. and Stern,L.J. (2008) *Immunology*, **123**, 305–313.
Wang,Y., Rubtsov,A., Heiser,R., White,J., Crawford,F., Marrack,P. and Kappler,J.W. (2005) *Proc. Natl Acad. Sci. U S A*, **102**, 2476–2481.
Wen,F., Esteban,O. and Zhao,H. (2008a) *J. Immunol. Methods*, **336**, 37–44.
Wen,F., McLachlan,M. and Zhao,H. (2008b) In Begley,T.P. (ed), *Wiley Encyclopedia of Chemical Biology*. John Wiley & Sons, Inc., Hoboken, NJ, pp. 1–10.
Wen,F., Rubin-Pitel,S. and Zhao,H. (2009) In Park,S. and Cochran,J.R. (eds), *Protein Engineering and Design*. CRC Press, Taylor & Francis Group, Boca Raton, FL, pp. 153–177.
Wucherpfennig,K.W., Sette,A., Southwood,S., Oseroff,C., Matsui,M., Strominger,J.L. and Hafler,D.A. (1994) *J. Exp. Med.*, **179**, 279–290.